International Immunopharmacology 75 (2019) 105766

Contents lists available at ScienceDirect

International Immunopharmacology

journal homepage: www.elsevier.com/locate/intimp

Interleukin-9 promotes tumorigenesis through augmenting angiogenesis in non-small cell lung cancer

Jun He[a,b], Li Wang[a,1], Chengda Zhang[c], Wenbin Shen[d], Yong Zhang[a], Tao Liu[e], Haoyue Hu[a], Xiaoxiao Xie[a], Feng Luo[a,*]

[a] Lung Cancer Center, West China Hospital, Sichuan University, Chengdu, Sichuan 610000, China
[b] Department of Oncology, The Third Hospital of Mianyang (Sichuan Mental Health Center), Mianyang, Sichuan 621000, China
[c] Department of Gastroenterology, The Third Hospital of MianYang (Sichuan Mental Health Center), Mianyang, Sichuan 621000, China
[d] Department of Radiotherapy, The Fourth Hospital of Hebei Medical University, Shijiazhuang, Hebei 050011, China
[e] Department of Oncology, The First Affiliated Hospital of Chengdu Medical College, Chengdu, Sichuan 610000, China

ARTICLE INFO

Keywords:
Interleukin-9
Non-small cell lung cancer
Angiogenesis
VEGF

ABSTRACT

IL-9 is a proinflammatory cytokine that plays a critical role in autoimmunity and inflammatory diseases. However, its role in tumorigenesis has not been well studied. In this study, we found that IL-9 expression was significantly increased and associated with poor progression in human non-small cell lung cancer (NSCLC). Ectopic expression of IL-9 in NSCLC cells did not affect cell proliferation and apoptosis *in vitro*, but markedly promoted tumor growth *in vivo*. Immune-profile analysis showed no significant changes in the frequencies of infiltrated immune cells in the tumor site, neither in nude mice nor in immune-competent mice. However, we found that VEGF and microvessel density (MVD) were significantly increased in xenografts. IL-9 could promote cell growth and tube formation of HUVEC cells *in vitro*. In addition, correlation analysis implied a significant positive relationship between the density of IL-9 and VEGF, as well as MVD in human NSCLC tissues. Finally, we found that IL-9 stimulated tumor angiogenesis *via* STAT3 signaling. Together, our findings demonstrate a promoting role of IL-9 in lung cancer development, probably through promoting tumor angiogenesis. IL-9 thus may represent a new prognostic marker and therapeutic target for NSCLC.

1. Introduction

Interleukin-9 (IL-9) was first cloned in 1989 as a member of the common cytokine receptor gamma chain-dependent family of cytokines, which also includes IL-2, IL-4, IL-7, IL-15 and IL-21 [1,2]. IL-9 is produced by a variety of cells, including mast cells, NKT cells, Th2, Th17, Treg, innate lymphoid cells (ILC) 2, and Th9 cells [3]. Among them, Th9 cells are regarded as the major $CD4^+$ T cells that produce IL-9. This IL-9-producing T cells generated with the cytokines TGF-β and IL-4 are characterized as a new T helper subset termed Th9 to distinguish them from classical Th2 cells [4,5].

As a proinflammatory cytokine, IL-9 is historically believed to be involved in type 2 immune responses and plays a critical role in autoimmune diseases and allergic inflammation [2,6]. IL-9 functions through the IL-9 receptor (IL9R), which activates different signal transducer and activator (STAT) proteins, including STAT1, STAT3, and STAT5, and thus connects this cytokine to various biological processes, including tumorigenesis [7].

The role of IL-9 in tumor development has been previously explored. Renauld and colleagues reported that IL-9 transgenic mice could develop thymic lymphomas [8]. IL-9 has been found upregulated in various human hematological tumors, including NK/T- cell lymphoma, Hodgkin's lymphoma, and large cell anaplastic lymphoma, and appears to be a negative prognostic factor [9–11]. Several studies have indicated that IL-9 promotes oncogenesis in human diffuse large B cell lymphoma [12], chronic lymphocytic leukemia [13], and large cell anaplastic lymphoma [14]. Recently report showed that IL-9 promoted pancreatic cancer cells proliferation and migration [15]. In addition, an animal study demonstrated that tumor growth was significantly inhibited in IL-9 deficient mice or neutralizing of IL-9 [16]. However, IL-9 also showed anti-tumor effect. One report revealed that ectopic expression of the membrane-bound IL-9 on tumor cells inhibited tumor

* Corresponding author at: Lung Cancer Center, West China Hospital of Sichuan University, NO. 363, Third Section of Furong Road, Yongning Town, Wenjiang District, Chengdu, Sichuan 610000, China.
E-mail address: hxyyluofeng@sina.com (F. Luo).
[1] Equal contribution.

https://doi.org/10.1016/j.intimp.2019.105766
Received 30 March 2019; Received in revised form 23 June 2019; Accepted 15 July 2019
Available online 25 July 2019

growth in colon cancer [17]. Fang et al. found that IL-9 inhibited melanoma cell growth through upregulation of p21 and TRAIL *in vitro* [18]. Therefore, IL-9 may play a pathogenic role in cancer. However, the function of IL-9 in tumorigenesis remains poorly studied.

IL-9 has been reported associated with the pathogenesis of multiple inflammatory diseases in the lung. Increased IL-9 production in the lung results in bronchial hyperresponsiveness and airway inflammation [19,20]. IL-9 can reduce lung fibrosis induced by silica particles in mice [21]. However, the role of IL-9 in lung cancer remains largely unknown. In this study, we evaluated the IL-9 expression in human non-small cell lung cancer (NSCLC) and explored its role in tumorigenesis using IL-9 over-expressing lung cancer cells and mice model. Our results show that IL-9 plays a promoting role in NSCLC by enhancing tumor angiogenesis.

2. Material and method

2.1. Specimens

Frozen and paraffin-embedded NSCLC tissue samples were collected from 56 patients who had been diagnosed with NSCLC and received surgery from January 2013 to December 2013 at the Department of Oncology, The Third Hospital of Mianyang. All participants have provided written consent. The study and consent procedure was approved by the Institutional Ethics Committee at The Third Hospital of Mianyang. The clinicopathologic characteristics of all patients were shown in Table 1.

2.2. Immunohistochemistry and evaluation

IL-9, VEGF, and CD31 expression were determined using IHC staining as described previously [22]. Briefly, paraffin sections were dewaxed, pretreated with 3% hydrogen peroxide to inactivate endogenous peroxidase, and antigen retrieved in citrate, then blocked with 5% normal goat serum. The sections were incubated with the rabbit anti-human IL-9 antibody (17689-1-AP, 1:50, Proteintech, Rosemont, IL, USA), or, rabbit anti-human CD31 antibody (ab134168, 1:300 dilution, Abcam, Cambridge, MA, USA), or mouse anti-human VEGFA antibody (ab1316, 1:500 dilution, Abcam, Cambridge, MA, USA), at 4 °C overnight, followed by horseradish peroxidase (HRP)-labeled anti-rabbit or anti-mouse IgG. Peroxidase activity was visualized by utilizing 3,3′ diaminobenzidine substrate according to the kit instructions (Beyotime Bio-science, Shanghai, China). Sections were then counterstained with hematoxylin. Slides were examined using a microscope (Eclipse E600; Nikon).

The positively stained cells were counted and scored with the formula: the percentage of positive cells × staining intensity. The staining intensity was scored as follows: 0 = no staining; 1 = light yellow; 2 = brownish yellow; and 3 = brown. The percentage of positive cells was scored as follows: 0 (< 10%), 1 (11%–25%), 2 (26%–50%), 3 (51%–75%) and 4 (> 76%). Total score of ≥4 was defined as a high expression, and a score of 0–3 was defined as low expression. MVD was recorded by counting CD31-positive immunostained endothelial cells [23]. The average of three 200× field microvessel counts was recorded as the value of MVD.

Table 1
Correlation between intratumoral IL-9 expression and clinicopathological variables in NSCLC patients.

Variables	Cases (56)	IL-9 expression		P value
		High (41)	Low (15)	
Age (years)				
≤60	35	25	10	0.697
> 60	21	16	5	
Gender				
Male	40	28	12	0.513
Female	16	13	3	
Histological type				
Adenocarcinoma	33	23	10	0.689
Squamous cell carcinoma	16	13	3	
others	7	5	2	
Smoking status				
Smoker	38	29	9	0.446
Non-smoker	18	12	6	
Differentiation				
High-moderate	13	11	2	0.477
Low	43	30	13	
Tumor status				
T1-T2	42	34	8	0.024
T3-T4	14	7	7	
TNM stage				
I–II	40	33	7	0.013
III	16	8	8	
Vascular invasion				
Yes	37	29	8	0.100
No	19	12	7	

2.3. Cell culture and transfection

Human lung cancer cell line H1299, A549, H1975, H1395, LLC1 mouse lung cancer cell line, and human umbilical vein endothelial cells (HUVEC) were purchased from the American Type Culture Collection (ATCC; Rockville, MD, USA) and cultured in DMEM (GIBCO, Shanghai, China) supplemented with 10% FBS, and maintained at 37 °C in a humidified condition of 95% air and 5% CO2. For HUVEC cells, 50 μg/ml Endothelial Cell Growth Supplement (BD Biosciences, Cat: 354006) was added for well growth. Full-length clone cDNA of human IL-9 (BC066285, Sino Biological, Beijing, China) or mice IL-9 (NM_008373.1, Sino Biological, Beijing, China) were cloned into a pLenti6.3-IRES2-EGFP lentiviral vector (Invitrogen, Carlsbad, CA, USA) to generate pLenti6.3-h(m)IL-9-IRES2-EGFP. pLenti6.3-IRES2-EGFP lentivirus was used as a negative control. H1299 or LLC1 cells were infected with the recombinant lentivirus carrying h(m) IL-9 at a multiplicity of infection (MOI) of 10. GFP-positive monoclonal cells were sorted into 96-well plates by FACS Aria III flow cytometer (BD, San Jose, USA), and amplified to stable clones. Stably transfected clones were validated by western blotting and ELISA. MISSION esiRNA targeting human STAT3 (Cat: EHU122051) and scrambled siRNA were purchased from Sigma (Sigma, St Louis, MO, USA). H1299 cells were transfected with STAT3 esiRNA or scrambled siRNA using Lipofectamine™ 2000 (Invitrogen™ Life Technologies) and evaluated after 48 h by Western blotting.

2.4. Cell viability assay

Cell viability was measured using an MTT Cell Proliferation and Cytotoxicity Assay kit (Beyotime Institute of Biotechnology, Haimen, China). 1×10^4 cells were seeded into 96-well plates and cultured for 24, 48 and 72 h, followed by the addition of MTT solution to the cells for 4 h. Subsequent to the removal of the medium, the remaining MTT formazan crystals were solubilized in DMSO and analyzed at 560 nm using a microplate reader (Benchmark Electronics, Inc., Angleton, TX, USA).

2.5. Cell apoptosis assay

Cells were harvested and washed in cold PBS prior to staining using an Apoptosis Detection kit (BD Biosciences, San Jose, CA, USA), according to the manufacturer's protocol. Briefly, 1×10^5 cells were resuspended in 500 μl binding buffer and stained with fluorescein isothiocyanate-conjugated Annexin V and propidium iodide. The samples were analyzed by flow cytometry (BD FACSCanto, BD Bioscience, San

Diego, CA, USA), and analyzed using Flowjo software (FlowJo, Ashland, OR, USA).

2.6. Tube formation assay

HUVEC cells were treated with conditioned medium (50%, v/v) from IL-9 or mock transfected H1299 cells for 8 h in the presence of recombinant Human (rh) IL-9 (50 ng/ml, Cat: 209-ILB-010, R&D Systems, USA) or anti-IL-9 (10 μg/ml, Cat: MAB2092-SP, R&D Systems, USA). The cells were then harvested and washed with PBS, and plated onto the layer of Matrigel (BD Bioscience, San Diego, CA, USA) at a density of 1×10^4 cells/well. Tubular structures were quantified and photographed under a microscope after 24 h.

2.7. Elisa

IL-9 levels from the culture medium of IL-9 transfected H1299 cells, mock-transfected and normal H1299 cells were measured using human IL-9 ELISA kit (Cat: DY209-05, R&D Systems, USA) according to the manufacturer's protocol. VEGF levels from the culture medium of IL-9 transfected H1299 cells were quantified using human VEGF ELISA kit (Cat: DVE00, R&D Systems, USA) according to the manufacturer's protocol. Serum IFN-γ and TNF-α levels from mice were measured using mouse IFN-γ (DY485-05, R&D Systems, USA) and TNF-α (DY410-05, R &D Systems, USA) ELISA kit according to the manufacturer's protocol.

2.8. RNA extraction and real-time PCR

RNA was extracted from human NSCLC tissues using Trizol (Invitrogen, Carlsbad, CA, USA) method and reverse transcripted to cDNA using M-MLV reverse transcriptase (Invitrogen). Expression of mRNA of IL-9 was analyzed by applying the quantitative reverse-transcription PCR (Takara, Kyoto, Japan) and SYBR green detection (Takara). The primers used are as followed: IL-9 forward: 5′-CTCTGT TTGGGCATTCCCTCT-3′ and reverse: 5′- GGGTATCTTGTTTGCATGG TGG-3′; β-actin forward: 5′- AGCTTCCAGACACGCTATCAT-3′ and reverse: 5′- CGGTACAACGAGCTGTTTCTAC-3′. The expression level of IL-9 was normalized to the housekeeping gene β-actin using the comparative threshold cycle ($2^{-\Delta\Delta Ct}$) method.

2.9. Western blot analysis

The NSCLC tissues or cells were harvested, lysed and 20 μg of total protein was separated by electrophoresis using 12% SDS-PAGE, transferred onto polyvinylidene fluoride membranes, pre-blocked with 5% skim milk for 90 min at room temperature and then incubated using the primary antibodies including rabbit anti-human IL-9 antibody (ab111915, 1:1000 dilution, Abcam, Cambridge, MA, USA), rabbit anti-human STAT3 (ab109085, 1:2000 dilution, Abcam), rabbit anti-human STAT3 (phospho S727) (ab32143, 1:2000 dilution, Abcam), and β-actin (ab119716, 1:1000 dilution, Abcam) overnight at 4 °C. the horseradish peroxidase (HRP)-conjugated seconded IgG antibody was applied for 1 h at room temperature. The bands were visualized using BioImaging Systems (UVP Inc., Upland, CA, USA).

2.10. In vivo tumor model

6–8 weeks old female BALB/C nude mice and C57BL/6 mice (Hebei Medical University, Shijiazhuang, China.) were maintained in the Laboratory for Animal Experiments under specified pathogen-free conditions. 5×10^6 IL-9 transfected H1299, or 1×10^6 IL-9 transfected LLC1 cells, or their corresponding mock-transfected cells in 100 μl PBS were injected subcutaneously into the flank region of nude mice or C57BL/6 mice, respectively. Anti-VEGF antibody (bevacizumab, Roche, Switzerland) was administered i.p. in PBS at 5 mg/kg twice a week for 2 weeks. Tumor growth was monitored every week. Tumor volume was measured using fine digital calipers and was calculated by the following formula: tumor volume = $0.5 \times \text{width}^2 \times \text{length}$. 4 weeks after tumor cell injection, mice were sacrificed, tumors were separated into two equal parts: one was fixed in 10% formalin, and embedded in paraffin, for Ki67 and TUNEL staining using immunohistochemistry, the other was used for flow cytometry. All procedures involving animals were approved by the Animal Care and Use Committee of Hebei Medical University. The experimental manipulation of mice was conducted in accordance with the National Institutes of Health Guide for the Care and Use of Laboratory Animals.

2.11. Immune-profile analysis by flow cytometry

Freshly transplanted tumors were scissored into small pieces and placed in 1 ml cell dissociation solution (100 U/ml collagenase IV and 100 μg/ml DNase IV (all from Sigma-Aldrich, USA) in RPMI-1640 with 10% FBS) with shaking at 80 rpm in 37 °C for 30 min, then filtered suspension through 70-micron filter. Centrifuged the supernatant at 400*g* for 5 min and re-suspended cells in 40% Percoll (Cat: 17-0891-01, GE Healthcare, Piscataway, NJ, USA), and centrifuged at 325*g* at RT for 20 min. Collected the cells at the bottom and depleted red blood cells using ACK buffer. The cells were washed and re-suspended in FACS staining buffer (PBS with 2% FBS). The fluorescence Abs used for FACS staining including FITC anti-mouse CD45 (Cat: 147710), PerCP/Cyanine5.5 anti-mouse CD3 (Cat: 100218), PE anti-mouse DX5 (Cat: 108908), PE/Cy7 anti-mouse CD11c (Cat: 117318), Brilliant Violet 510 anti-mouse F4/80 (Cat: 123135), APC anti-mouse/human CD11b (Cat: 101211), APC/Cyanine7 anti-mouse Gr-1 (Cat: 108424), APC anti-mouse CD4 (Cat: 100412), PE/Cy7 anti-mouse CD8 (Cat: 100722). All Abs were purchased from BioLegend (San Diego, CA, USA). Dead cells were excluded using Sytox blue dead cell staining (Cat: S34857, Invitrogen, Carlsbad, CA, USA). Flow cytometry was performed using BD FACSCanto II (BD Bioscience, San Diego, CA, USA), and analyzed using Flowjo software (FlowJo, Ashland, OR, USA).

2.12. Statistical analysis

Data are expressed as the mean ± standard deviation. Statistical analyses were performed using GraphPad Prism 7 software (GraphPad Software, San Diego, CA). Overall survival (OS) was defined as the interval between surgery and death. Kaplan-Meier survival curve was plotted for the analysis of survival rates with a log-rank test. Inter-group statistical significance was determined using a Student's unpaired *t*-test. $P < 0.05$ was considered statistically significant.

3. Results

3.1. Increased IL-9 expression is associated with poor progression in human NSCLC

IL-9 expression has been found increased in numerous tumors, however, its expression in NSCLC has not been reported. Here, we measured the mRNA and protein levels of IL-9 in 56-paired NSCLC tissues. As shown in Fig. 1A and B, NSCLC tissues had significantly increased mRNA and protein levels of IL-9, compared with adjacent normal tissues. Immunohistochemical staining indicated that NSCLC tissues showed strong (22/56) or moderate (19/56) positive staining, whereas the majority of normal lung tissues were negative (42/56), only 14 cases showed weekly staining (Fig. 1D, $P < 0.01$).

To investigate the prognostic value of IL-9 in NSCLC patients, OS was assessed for patients with high ($n = 41$) and low ($n = 15$) IL-9 expression by Kaplan-Meier survival analysis. The results showed that patients with high IL-9 expression presented shorted overall survival (Fig. 1E, $P = 0.007$). The results were validated by an online database (http://kmplot.com/analysis/) (Fig. 1F). Taken together, our results suggest that increased IL-9 expression is associated with poor

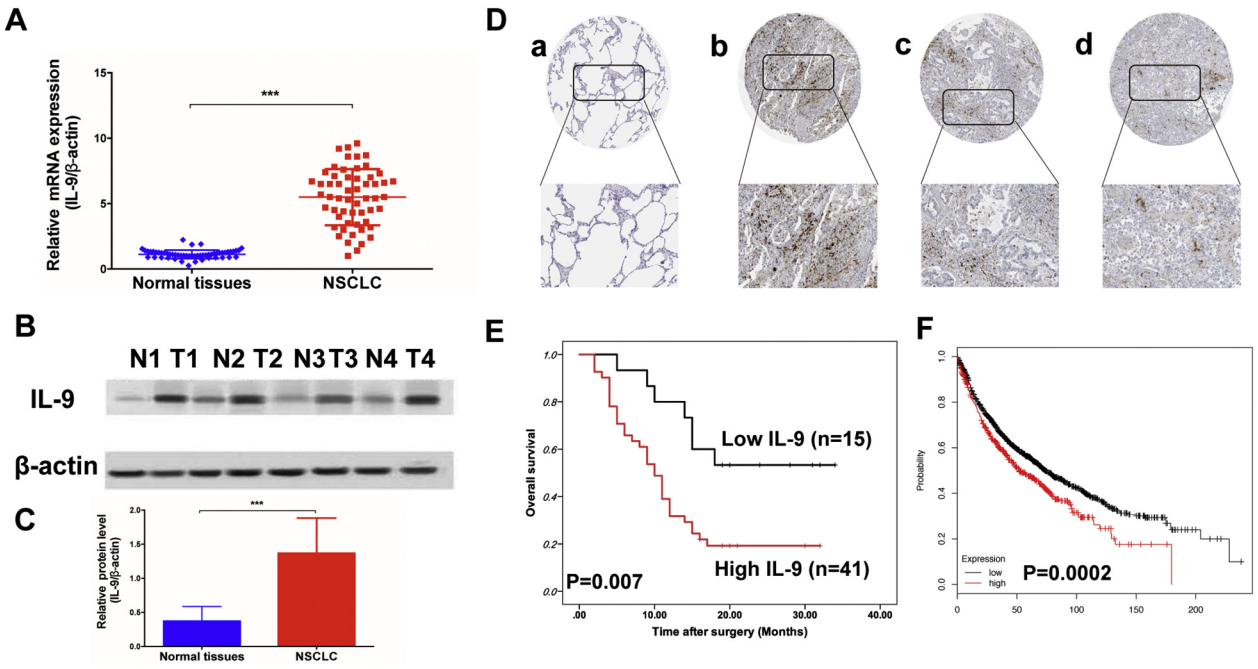

Fig. 1. Increased IL-9 expression is associated with poor progression in human NSCLC. qRT-PCR (A), and western blot (B–C) analysis of the expression of IL-9 in 56 paired of NSCLC samples and corresponding normal lung tissues. Depicted are 4 individual pairs of NSCLC samples. (D) Immunohistochemistry staining of human NSCLC sections using anti-IL-9 antibody. Negative (a) staining in normal lung tissue; high (b), moderate (c), and low (c) staining in NSCLC tissues. Magnification: ×100 (upper) and ×200 (lower). (E) Kaplan-Meier curves of survival differences among NSCLC patients with high IL-9 expression (n = 41) and low IL-9 expression (n = 15) after surgery. (F) Kaplan-Meier survival curves for overall survival according to IL-9 expression in an online database of NSCLC patients (http://kmplot.com/analysis/), red line, high IL-9 expression (n = 513); black line, low IL-9 expression (n = 1413). P values were determined by the log-rank test. Data shown are mean ± SD. ***P < 0.001. (For interpretation of the references to colour in this figure legend, the reader is referred to the web version of this article.)

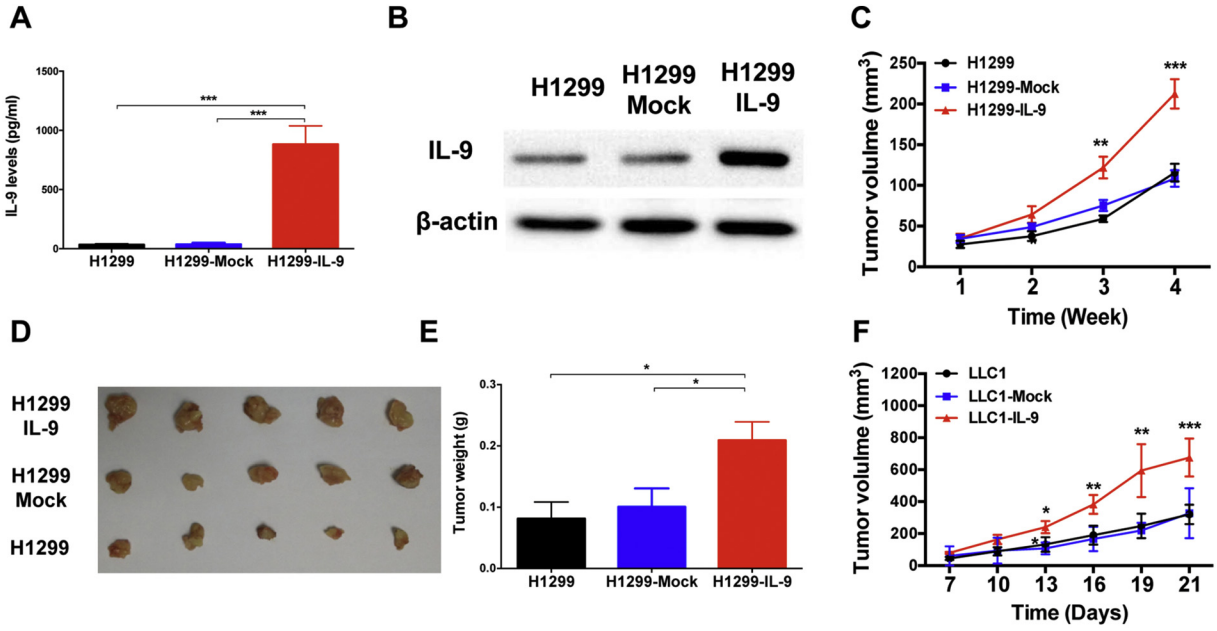

Fig. 2. IL-9 promotes NSCLC tumorigenesis *in vivo*. ELISA (A) and western blot (B) analysis of IL-9 expression from normal H1299, mock transfected, and IL-9 transfected H1299 cells. 5×10^6 IL-9 transfected H1299 or their corresponding mock-transfected cells were injected subcutaneously into the flank region of nude mice. Tumor growth was monitored every week. Tumor growth curves (C), photographs of xenografts (D), and tumor weight (E) of three groups were shown (n = 5 per group). (F) 1×10^6 IL-9 transfected LLC1 cells or their corresponding mock-transfected cells were injected subcutaneously into the flank region of C57BL/6mice. Tumor growth curves were shown. Data shown are mean ± SD from three independent experiments. *P < 0.05, **P < 0.01, ***P < 0.001.

progression in human NSCLC, IL-9 maybe exert an oncogenic role in NSCLC.

3.2. IL-9 promotes NSCLC tumorigenesis in vivo

It has been shown that IL-9 is the cytokine majorly expressed by immune cells, not in tumor cells. In order to investigate the effect of intracellular IL-9 on lung tumor progression, we first examined the IL-9

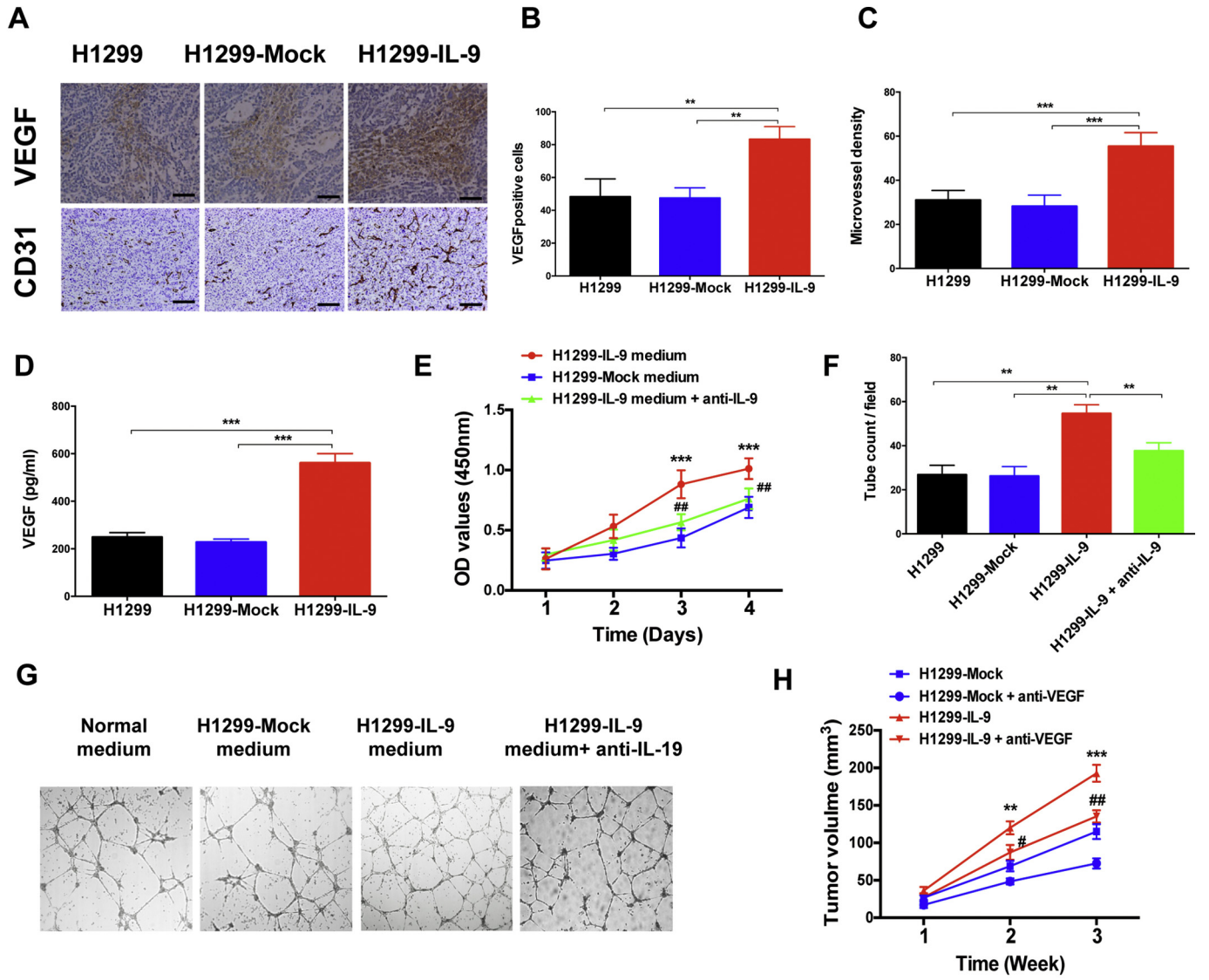

Fig. 3. IL-9 promotes tumor angiogenesis *in vitro* and *in vivo*. (A–B) VEGF and (A–C) CD31 expression levels in tumor sections from normal H1299, mock transfected, and IL-9 transfected H1299 cells were determined by IHC. Representative pictures are shown. (D) Levels of VEGF in normal H1299, mock transfected, and IL-9 transfected H1299 cells were measured by ELISA. (E) Conditional medium (1/2) from IL-9 or mock transfected H1299 cells were used to treat HUVEC cell. Anti-IL-9 (10 μg/ml) was added as described in methods. Cell growth was determined by CCK-8 assay. (F and G) Capillary structure formation was measured using matrigel tubule formation assay. Representative pictures and counted numbers are shown. Data shown are mean ± SD from three independent experiments. $^{**}P < 0.01$, $^{***}P < 0.001$, compared with group of H1299-IL-9 medium; $^{\#\#}P < 0.01$, compared with group of H1299-IL-9 medium + anti IL-9 (H) 5×10^6 IL-9 transfected H1299 or their corresponding mock-transfected cells were injected subcutaneously into the flank region of nude mice. Anti-VEGF antibody (bevacizumab, Roche, Switzerland) was administered i.p. in PBS at 5 mg/kg twice a week for 2 weeks. Tumor growth was monitored every week. Tumor growth curves were shown (n = 6 per group). Data shown are mean ± SD from three independent experiments. $^{*}P < 0.05$, $^{**}P < 0.01$, $^{***}P < 0.001$, compared with H1299-Mock group; $^{\#}P < 0.05$, $^{\#\#}P < 0.01$, compared with H1299-IL-9 + anti-VEGF group.

level in lung cancer cell lines. We found that lung tumor cells did not secret IL-9 or at very low levels (Fig. S1A). We therefore established H1299 cells line that stably expressing human IL-9. ELISA and Western blot showed abundant IL-9 expression in IL-9 transfected H1299 cells, compared with mock-transfected and WT cells (Fig. 2A and B). We then evaluated the cell growth, cell apoptosis as well as cell cycle *in vitro*. We first confirmed that HCT119 cells had higher levels of IL-9 receptor on the membrane using flow cytometry, indicating that it can respond to IL-9 signaling (data not shown). As shown in Fig. S1B–D, no significant differences in cell growth, cell apoptosis and cell cycle among the three groups. Similar results were confirmed by using another NSCLC cell line A549 that stably express IL-9 (Fig. S2A–C). In addition, we found that treatment of NSCLC cells with recommendation IL-9 or neutralizing antibody against IL-9 also had no effect on tumor proliferation or apoptosis *in vitro* (Fig. S1E–F). Taken together, our results suggest that IL-9 may not directly affect cell growth and apoptosis of NSCLC cells *in vitro*.

However, after we transplanted IL-9 transfected H1299 cells or A549 cells into nude mice, IL-9-expressing cells grew faster than mock-transfected or WT cells (Figs. 2C and S2D). The mean tumor weights of the IL-9-transfected xenografts were markedly larger than mock-transfected and WT xenografts 4 weeks after transplantation (Fig. 2D and E). In addition, Ki67 and TUNEL staining exhibited similar cell proliferation and cell apoptosis rate of xenografts between three groups (Fig. S1G–I). Therefore, our data indicate that IL-9 promotes NSCLC growth *in vivo*, but maybe not through regulating tumor growth and apoptosis directly.

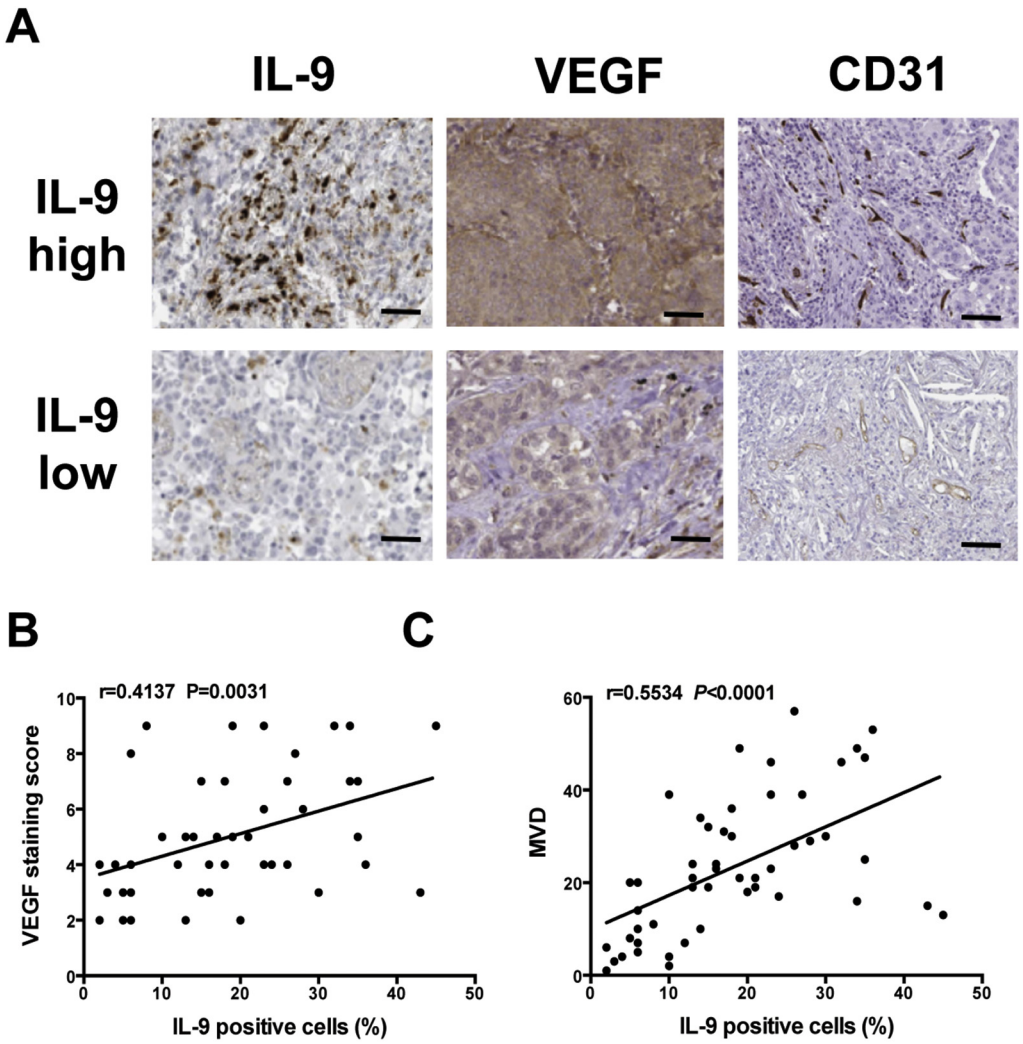

Fig. 4. IL-9 is positively associated with angiogenesis in NSCLC patients. (A) Representative immunohistochemical staining of IL-9, VEGF, and CD31 in the tumor sections from patients with high or low expression of IL-9. (B and C) The relationship between the density of IL-9-positive cells and VEGF, as well as MVD. Spearman's rank correlation coefficient.

3.3. IL-9 does not alter immune cell responses in vivo

Since IL-9 is a pleiotropic cytokine that plays an important role in immune responses. We analyzed the frequencies of immune cells in H1299 xenografts. As shown in Fig. S3A, similar cell populations of NK cells, DCs, macrophages, as well as MDSCs were found among three groups. In addition, serum IFN-γ and TNF-α were also showed similar levels between IL-9 and mock-transfected xenografts (Fig. S3B–C). These findings suggest that IL-9 does not affect tumor immunity *in vivo*. While nude mice do not have T or B cells, it prevents us to evaluate the anti-tumor T cells responses by IL-9 *in vivo*. We then generated IL-9 stably transfected LLC1 murine lung cancer cells. IL-9 overexpression also did not affect LLC1 cells proliferation and apoptosis *in vitro* (Data not shown). However, once the IL-9 transfected LLC1 cells were transplanted into C57BL/6 mice, it also showed significantly slower tumor growth than mock-transfected cells and WT cells (Fig. 2F). Immune-profile analysis showed that the proportions of $CD3^+T$, $CD4^+T$, $CD8^+T$, as well as NK cells were comparable between two groups (Fig. S3D). Serum levels IFN-γ and TNF-α were also showed similar levels between the three groups (Fig. S3E–F). Taken together, these results reveal that IL-9 does not alter immune cell responses *in vivo*.

3.4. IL-9 promotes tumor angiogenesis in vitro and in vivo

Previous study showed that IL-9 could induce angiogenesis in psoriasis-like skin inflammation [24], suggesting that IL-9 may promote NSCLC growth through modulating tumor angiogenesis. We first examined the two angiogenic markers VEGF and CD31 expressions in xenografts sections. The results showed that IL-9 significantly increased VEGF and CD31 staining, and more tumor blood vessels (MVD) were observed in IL-9 transfected xenografts compared with mock-transfected xenografts (Fig. 3A–C). ELISA assay found that IL-9 transfected H1299 cells secreted more VEGF than mock-transfected cells (Fig. 3D). We then used the conditioned medium (50%, *v*/v) from IL-9 or mock transfected H1299 cells to treat HUVEC cells. We found that the cell growth (Fig. 3E) and tube formation (Fig. 3F and G) of HUVEC cells were significantly increased after treated with IL-9 transfected H1299 cells medium. However, the effects could be reversed by adding neutralizing antibody against IL-9 (Fig. 3E–G). To further confirm that IL-9 promotes tumor growth through enhancing angiogenesis, we used anti-VEGF antibody to block the tumor angiogenesis *in vivo* during IL-9 overexpression. We found that IL-9 could not promote tumor growth after blocking tumor angiogenesis *in vivo* (Fig. 3H). Collectively, these results indicate that IL-9 might promote NSCLC progression through directly regulating tumor angiogenesis *in vitro* and *in vivo*.

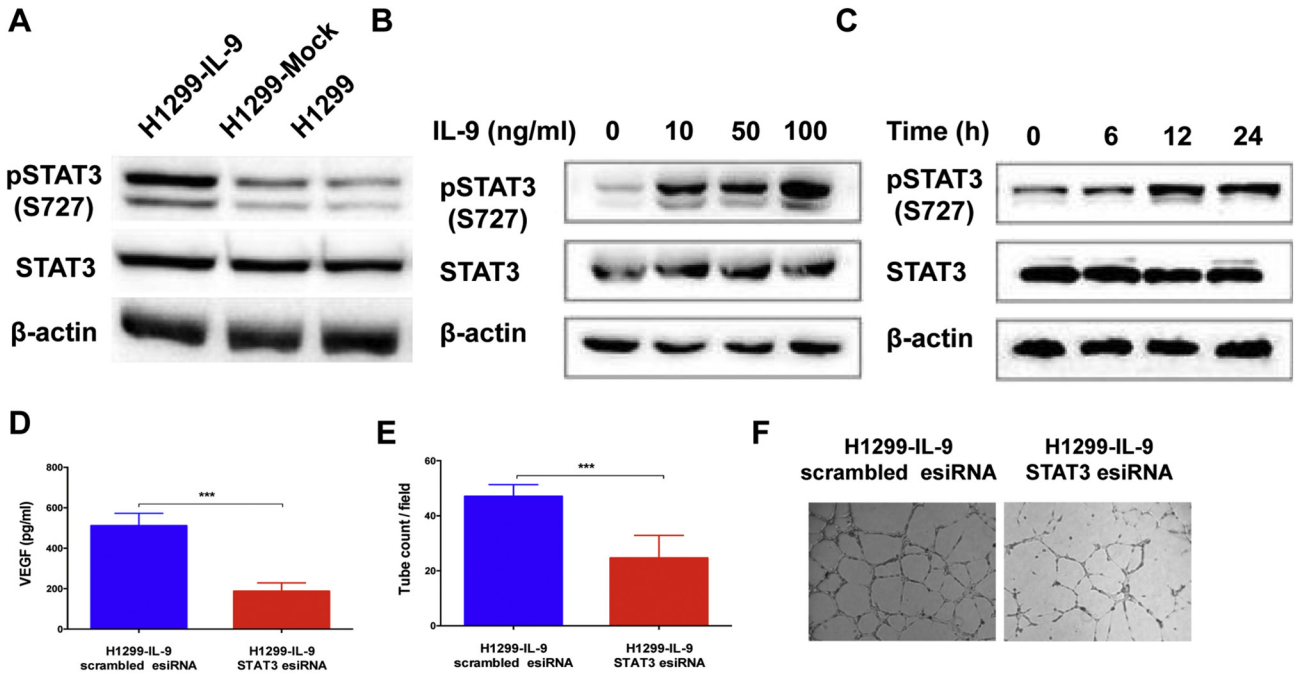

Fig. 5. IL-9 stimulates angiogenesis *via* STAT3. (A) Western blotting showed that phosphorylation of STAT3 was obviously increased in IL-9 transfected H1299 cells. (B-C) H1299 cells were incubated with rhIL-9 at the indicated concentrations for 24 h or at 100 ng/ml for the indicated time. Phosphorylation of STAT3 was examined by western blotting. (D) Levels of VEGF in IL-9 transfected H1299 cells or STAT3 knockdown IL-9 transfected H1299 cells were measured by ELISA. (E–F) Medium from IL-9 transfected H1299 cells or STAT3 knockdown IL-9 transfected H1299 cells were harvested, HUVECs were seeded in 96-well plates coated with matrigel and treated with conditional medium (50%) for 16 h. Tubular structures were photographed and tube length was measured. Data shown are mean ± SD from three independent experiments. ***P < 0.001.

3.5. IL-9 is positively associated with angiogenesis in NSCLC patients

We next evaluated the relationship between IL-9 and tumor angiogenesis in human NSCLC tissues. The results showed that patients with high IL-9 expression had strong VEGF and CD31 staining (Fig. 4A). Correlation analysis indicated a significant positive relationship between the density of IL-9-producing cells and VEGF ($r = 0.4137$, $P = 0.0031$, Fig. 4B), as well as MVD ($r = 0.5534$, $P < 0.0001$, Fig. 4C), suggesting that IL-9 is positively associated with tumor angiogenesis in NSCLC patients.

3.6. IL-9 stimulates angiogenesis via STAT3

Accumulating evidence suggests that signal transducer and activator of transcription (STATs), mainly STAT3, play an important role in angiogenesis [25]. In addition, IL-9-mediated signal transduction results in the activation of STAT1, STAT3, and STAT5 [26]. We then explore whether IL-9 mediated tumor angiogenesis is *via* activation of STAT3 in NSCLC cells. We found that IL-9 transfected H1299 cells showed increased pSTAT3 levels compared with mock-transfected cells (Fig. 5A). In addition, recombinant human IL-9 treatment also increased phosphorylation of STAT3 in a time and dose-dependent manner (Fig. 5B and C).

We then used siRNA to knockdown of STAT3 expression in IL-9 or mock transfected H1299 cells and then explored the role of STAT3 in IL-9 medicated effects on tumor angiogenesis. As shown in Fig. 5D, knockdown of STAT3 inhibited VEGF expression in IL-9 transfected H1299 cells. Treatment of conditional medium from STAT3 knockdown IL-9 transfected H1299 cells repressed tube formation of HUVECs (Fig. 5E and F). The results were also confirmed by using STAT3 inhibitor S3I-201 (Fig. S4A–C). Taken together, these results suggest that IL-9 stimulates tumor angiogenesis partially through STAT3 signaling.

4. Discussion

IL-9 has been found with various functions in different tumors [9,11,15,18]. However, the role of IL-9 in tumorigenesis remains poorly understood. In this study, by using human NSCLC samples and lung cancer xenograft models, we proposed a promoting role of IL-9 in NSCLC progression. We found that IL-9 is highly expressed in NSCLC tissues, and associated with poor outcome in human NSCLC. Besides, ectopic expression of IL-9 promoted *in vivo* tumor growth of H1299 cells. Therefore, our findings indicate that IL-9 plays a promoting role in the growth of human NSCLC.

IL-9 is considered to be a pleiotropic cytokine and involved in type 2 immune responses [6]. IL-9 signals through the JAK/STAT system, which induces the activation of STAT1, STAT3, and STAT5, and is involved in cell survival, proliferation and secretion of inflammatory mediators [3]. However, in the present study, we found that ectopic expression of IL-9 in NSCLC cells did not inhibit cell proliferation and apoptosis *in vitro*. IL-9 also has no effect on anti-immune responses *in vivo* both in nude mice and immune-competent mice. Our results were consistent with the results in colon carcinoma showed that IL-9 overexpression on tumor cells had no effect on cell proliferation or major histocompatibility complex class I expression [17], but inconsistent with previous studies showed that IL-9 could promote the proliferation, invasion, and migration of pancreatic cancer cells, as well as diffuse large B-cell lymphoma [27]. In contrast to the pro-tumor effect of IL-9, two studies demonstrated an anti-tumor effect of IL-9 in colon cancer and melanoma [17,18]. Therefore, further studies are needed to ascertain the role of IL-9 in tumorigenesis in more tumor models. In addition, our correlation analysis of NSCLS samples showed that IL-9 was highly expressed in the early status (T1-T2) and stage (I-II), indicating that IL-9 maybe already abundant at the early phase of tumorigenesis of NSCLS, probably due to the massive infiltration of lymphocytes at the early stage of tumor development. Therefore, IL-9 involvement is pivotal for the early phase of tumorigenesis and that its neutralization

might partially restrain the progression of tumor.

What's the mechanism underlying the promotion of NSCLC by IL-9? During the investigation, we found one report presented the pro-angiogenesis role of IL-9 in psoriasis-like skin inflammation [24], suggesting that IL-9 may promote NSCLC growth through modulating tumor angiogenesis, since angiogenesis is a critical process for the sustained growth of tumors *in vivo*. Indeed, we found that IL-9 overexpressed cells had increased VEGF levels; conditional medium from IL-9 transfected H1299 cells induced more tube formation of HUVEC cells. In addition, IL-9 transfected xenografts had increased VEGF levels and more MVD, which suggested enhanced angiogenesis *in vitro* and *in vivo*. We also confirmed our observation in clinical NSCLC tissues samples; there was a positive relationship between the density of IL-9 and VEGF as well as MVD. Since STAT3 is critical in both IL-9 and angiogenesis signaling [2,25], we found that IL-9 may stimulate angiogenesis partially through STAT3. Together, our data reveal a novel mechanism of IL-9 in tumorigenesis through promoting angiogenesis.

In summary, our finding demonstrate that IL-9 is highly expressed in NSCLC and associated with poor prognosis in NSCLC patients and plays a pro-tumor role in NSCLC progression through promoting tumor angiogenesis *via* STAT3. IL-9 thus may represent a useful prognostic marker and therapeutic target for NSCLC.

Supplementary data to this article can be found online at https://doi.org/10.1016/j.intimp.2019.105766.

Funding

This work was supported by the National Natural Science Foundation of China (No. 81802512) and the Health Commission of Mianyang City (No. 201706).

Declaration of Competing Interest

The authors declare that they have no competing interests.

References

[1] J. Van Snick, A. Goethals, J.C. Renauld, E. Van Roost, C. Uyttenhove, M.R. Rubira, R.L. Moritz, R.J. Simpson, Cloning and characterization of a cDNA for a new mouse T cell growth factor (P40), J. Exp. Med. 169 (1) (1989) 363–368.

[2] R. Goswami, M.H. Kaplan, A brief history of IL-9, J. Immunol. 186 (6) (2011) 3283–3288, https://doi.org/10.4049/jimmunol.1003049.

[3] P. Zhao, X. Xiao, R.M. Ghobrial, X.C. Li, IL-9 and Th9 cells: progress and challenges, Int. Immunol. 25 (10) (2013) 547–551, https://doi.org/10.1093/intimm/dxt039.

[4] M. Veldhoen, C. Uyttenhove, J. van Snick, H. Helmby, A. Westendorf, J. Buer, B. Martin, C. Wilhelm, B. Stockinger, Transforming growth factor-beta 'reprograms' the differentiation of T helper 2 cells and promotes an interleukin 9-producing subset, Nat. Immunol. 9 (12) (2008) 1341–1346, https://doi.org/10.1038/ni.1659.

[5] V. Dardalhon, A. Awasthi, H. Kwon, G. Galileos, W. Gao, R.A. Sobel, M. Mitsdoerffer, et al., IL-4 inhibits TGF-beta-induced Foxp3+ T cells and, together with TGF-beta, generates IL-9+ IL-10+ Foxp3(-) effector T cells, Nat. Immunol. 9 (12) (2008) 1347–1355, https://doi.org/10.1038/ni.1677.

[6] W.G. Rojas-Zuleta, E. Sanchez, IL-9: function, sources, and detection, Methods Mol. Biol. 1585 (2017) 21–35, https://doi.org/10.1007/978-1-4939-6877-0_2.

[7] L. Knoops, J.C. Renauld, IL-9 and its receptor: from signal transduction to tumorigenesis, Growth Factors 22 (4) (2004) 207–215, https://doi.org/10.1080/08977190410001720879.

[8] J.C. Renauld, N. van der Lugt, A. Vink, M. van Roon, C. Godfraind, G. Warnier, H. Merz, A. Feller, A. Berns, J. Van Snick, Thymic lymphomas in interleukin 9 transgenic mice, Oncogene 9 (5) (1994) 1327–1332.

[9] J. Zhang, W.D. Wang, Q.R. Geng, L. Wang, X.Q. Chen, C.C. Liu, Y. Lv, Serum levels of interleukin-9 correlate with negative prognostic factors in extranodal NK/T-cell lymphoma, PLoS One 9 (4) (2014) e94637, , https://doi.org/10.1371/journal.pone.0094637.

[10] M. Fischer, M. Bijman, D. Molin, F. Cormont, C. Uyttenhove, J. van Snick, C. Sundstrom, G. Enblad, G. Nilsson, Increased serum levels of interleukin-9 correlate to negative prognostic factors in Hodgkin's lymphoma, Leukemia 17 (12) (2003) 2513–2516, https://doi.org/10.1038/sj.leu.2403123.

[11] H. Merz, F.A. Houssiau, K. Orscheschek, J.C. Renauld, A. Fliedner, M. Herin, H. Noel, et al., Interleukin-9 expression in human malignant lymphomas: unique association with Hodgkin's disease and large cell anaplastic lymphoma, Blood 78 (5) (1991) 1311–1317.

[12] A.A. Aliev, N.A. Garanina, Liver exocrine function and lipid metabolism in the digestive tract of calves, Fiziol. Zh. SSSR Im. I M Sechenova 66 (2) (1980) 256–262.

[13] N. Chen, K. Lu, P. Li, X. Lv, X. Wang, Overexpression of IL-9 induced by STAT6 activation promotes the pathogenesis of chronic lymphocytic leukemia, Int. J. Clin. Exp. Pathol. 7 (5) (2014) 2319–2323.

[14] L. Qiu, R. Lai, Q. Lin, E. Lau, D.M. Thomazy, D. Calame, R.J. Ford, L.W. Kwak, R.A. Kirken, H.M. Amin, Autocrine release of interleukin-9 promotes Jak3-dependent survival of ALK+ anaplastic large-cell lymphoma cells, Blood 108 (7) (2006) 2407–2415, https://doi.org/10.1182/blood-2006-04-020305.

[15] B. Hu, H. Qiu-Lan, R.E. Lei, C. Shi, H.X. Jiang, S.Y. Qin, Interleukin-9 promotes pancreatic cancer cells proliferation and migration via the miR-200a/Beta-catenin axis, Biomed. Res. Int. 2017 (2017) 2831056, , https://doi.org/10.1155/2017/2831056.

[16] D.B. Hoelzinger, A.L. Dominguez, P.A. Cohen, S.J. Gendler, Inhibition of adaptive immunity by IL9 can be disrupted to achieve rapid T-cell sensitization and rejection of progressive tumor challenges, Cancer Res. 74 (23) (2014) 6845–6855, https://doi.org/10.1158/0008-5472.CAN-14-0836.

[17] V.A. Do Thi, S.M. Park, H. Lee, Y.S. Kim, Ectopically expressed membrane-bound form of IL-9 exerts immune-stimulatory effect on CT26 colon carcinoma cells, Immune Netw. 18 (1) (2018) e12, https://doi.org/10.4110/in.2018.18.e12.

[18] Y. Fang, X. Chen, Q. Bai, C. Qin, A.O. Mohamud, Z. Zhu, T.W. Ball, et al., IL-9 inhibits HTB-72 melanoma cell growth through upregulation of p21 and TRAIL, J. Surg. Oncol. 111 (8) (2015) 969–974, https://doi.org/10.1002/jso.23930.

[19] U.A. Temann, G.P. Geba, J.A. Rankin, R.A. Flavell, Expression of interleukin 9 in the lungs of transgenic mice causes airway inflammation, mast cell hyperplasia, and bronchial hyperresponsiveness, J. Exp. Med. 188 (7) (1998) 1307–1320.

[20] M.P. McLane, A. Haczku, M. van de Rijn, C. Weiss, V. Ferrante, D. MacDonald, J.C. Renauld, N.C. Nicolaides, K.J. Holroyd, R.C. Levitt, Interleukin-9 promotes allergen-induced eosinophilic inflammation and airway hyperresponsiveness in transgenic mice, Am. J. Respir. Cell Mol. Biol. 19 (5) (1998) 713–720, https://doi.org/10.1165/ajrcmb.19.5.3457.

[21] M. Arras, F. Huaux, A. Vink, M. Delos, J.P. Coutelier, M.C. Many, V. Barbarin, J.C. Renauld, D. Lison, Interleukin-9 reduces lung fibrosis and type 2 immune polarization induced by silica particles in a murine model, Am. J. Respir. Cell Mol. Biol. 24 (4) (2001) 368–375, https://doi.org/10.1165/ajrcmb.24.4.4249.

[22] Y. Wang, L. Tu, C. Du, X. Xie, Y. Liu, J. Wang, Z. Li, et al., CXCR2 is a novel cancer stem-like cell marker for triple-negative breast cancer, Onco Targets Ther. 11 (2018) 5559–5567, https://doi.org/10.2147/OTT.S174329.

[23] P.B. Vermeulen, G. Gasparini, S.B. Fox, C. Colpaert, L.P. Marson, M. Gion, J.A. Belien, et al., Second international consensus on the methodology and criteria of evaluation of angiogenesis quantification in solid human tumours, Eur. J. Cancer 38 (12) (2002) 1564–1579.

[24] T.P. Singh, M.P. Schon, K. Wallbrecht, A. Gruber-Wackernagel, X.J. Wang, P. Wolf, Involvement of IL-9 in Th17-associated inflammation and angiogenesis of psoriasis, PLoS One 8 (1) (2013) e51752, , https://doi.org/10.1371/journal.pone.0051752.

[25] Z. Chen, Z.C. Han, STAT3: a critical transcription activator in angiogenesis, Med. Res. Rev. 28 (2) (2008) 185–200, https://doi.org/10.1002/med.20101.

[26] J.H. Bauer, K.D. Liu, Y. You, S.Y. Lai, M.A. Goldsmith, Heteromerization of the gammac chain with the interleukin-9 receptor alpha subunit leads to STAT activation and prevention of apoptosis, J. Biol. Chem. 273 (15) (1998) 9255–9260.

[27] X. Lv, L. Feng, X. Ge, K. Lu, X. Wang, Interleukin-9 promotes cell survival and drug resistance in diffuse large B-cell lymphoma, J. Exp. Clin. Cancer Res. 35 (1) (2016) 106, https://doi.org/10.1186/s13046-016-0374-3.